The chemistry of planet-forming disks: a story from inner to outer disk

Temmink, M.

Chapter 1

Introduction

Questions that captivate many astronomers are "Where does life form?" and "Could there be life elsewhere in the Universe?" Presently, over 6,000 exoplanets have been discovered and, statistically speaking, it is expected that every star hosts at least one planet, making it nearly unthinkable that life has only ever thrived on Earth. To answer these questions and to determine whether the Earth is a unique case, we need to understand planets, the regions in which they form and how they evolve. Disks around young, newly-formed stars play a crucial role in answering these questions, as they are the cradles of planets and set their (chemical) composition.

With every passing day, our understanding of planet-forming disks grows, in part due to the active development of new telescopes and instruments. The field of planet-forming disks and the adjacent field of astrochemistry have undergone rapid developments over this past decade through new observations and insights from telescopes such as the Atacama Large Millimeter/submillimeter Array (ALMA; Wootten & Thompson 2009) and the *James Webb* Space Telescope (JWST; Rigby et al. 2023). This thesis uses these telescopes to make the next step in the investigation of the chemical composition of planet-forming disks.

1.1 Star- and planet-formation

To study planet-forming disks, one needs to understand the different phases of star- and planet-formation (see Shu et al. 1987, McKee & Ostriker 2007, Luhman 2012, and Tobin & Sheehan 2024 for elaborate reviews). The processes occur in molecular clouds, and the phases range from the initial collapse of dense cores to the formation of a disk, and, finally, a planetary system (see Figure 1).

Molecular clouds. Clouds are dense structures in the interstellar medium (ISM) that consist mainly of gas (99% of the mass) and a small fraction of silicate and carbonaceous dust grains (Draine 2003). The process of star-formation happens in the dense molecular clouds ($n_{\rm H}$ >10^3 cm^{-3}) that have low temperatures (Öberg

& Bergin 2021) and, as the name suggests, are mainly made up of molecules (see panel a of Figure 1).

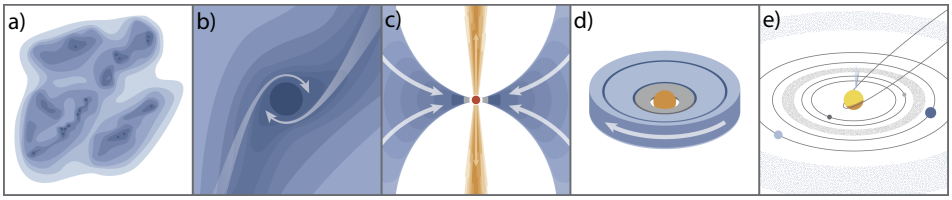

Figure 1.1: Different phases of star- and planet formation. Panel a) displays the molecular cloud with dense cores indicated by the dark blue regions. Panel b) marks the collapse of such a cloud core. Panel c) highlights the protostellar phase, indicating the accretion process, the formation of the disk, and outflowing material. Panel d) displays the planet-forming disks, and Panel e) shows the final stage, the remnant planetary system. This figure has been adopted from Öberg & Bergin (2021).

Pre-stellar cores. The molecular clouds consist of even denser regions ($n_{\rm H}$ $\sim$$10^4$-$10^5$ cm^{-3}), known as pre-stellar cores, with temperatures of $\sim$10 K (see Bergin & Tafalla 2007 for a review). Once the inward gravitational force of the core overcomes the outward (turbulent, magnetic, and thermal) pressure, the dense core collapses and a young protostar forms at its centre (see panel b of Figure 1).

Protostars. The stage of a young protostar is characterised by accretion, disk formation, and outflows and jets (see panel c of Figure 1). As the young star is still surrounded by material from its parent cloud, also known as the protostellar envelope, it can directly accrete this material to gain more mass. At the same time, a disk is formed around the young protostar to conserve the angular momentum of the system (Cassen & Moosman 1981). This also acts as a funnel, allowing the young protostar to accrete even more material. The protostellar outflows and jets act, on the other hand, as a means of removing angular momentum. This stage lasts for about a million years and ends once the envelope has dispersed.

Planet-forming disks. Once the protostellar envelope is dispersed, the young star, still surrounded by a disk, becomes visible. This stage is known as the planet-forming disk stage (see panel d of Figure 1) and is the topic of this thesis. During this phase, the star is still accreting mass from the disk, but planets are also actively forming (Williams & Cieza 2011). Although the onset of planet formation may already start in the earlier phases (Harsono et al. 2018; Tychoniec et al. 2020), the planets will be actively accreting material from the disk (both dust and gas), in turn shaping the disk's evolution.

Observationally, young stellar objects are divided into different classes. The most deeply embedded protostars are denoted as Class 0 objects, whereas the less embedded young protostars are denoted as Class I objects. Pre-main sequence stars surrounded by planet-forming disks, the topic of this thesis, are known as Class II objects. A final class, the Class III objects, are young stars which are surrounded by very little dust. These systems mark the final stage between a planet-forming disk and a full planetary system, such as the Solar System. Aside

from the different classes based on the star-formation stage, planet-forming disks themselves are subdivided into categories based on the mass and/or spectral type of their host stars. The lowest mass stars ($M_* \leq 0.2\ M_\odot$) are known as Very Low Mass Stars (VLMSs) and are empirically considered to be objects with spectral types equal to or later than M5 (Pinilla 2022), while the heavier stars ($1.5\ M_\odot \leq M_* \leq 10\ M_\odot$) with spectral types of F, A, and B are known as Herbig stars (Herbig 1960; Brittain et al. 2023). Stars with masses in between these limits and, therefore, have a similar mass as the Sun, are known as T-Tauri stars. The disks around each of these stars are thus known as VLMS disks, T-Tauri disks, and Herbig disks.

Planet-forming disks are, from a chemical point of view, also extremely interesting objects. Since they are a critical stage in between the cold molecular clouds and the emerging planetary systems, understanding the chemical composition and the ongoing chemical processes in disks is of key importance. One question that needs to be answered: is the chemistry in planet-forming disks a result of inheritance of the earlier phases, or has a chemical reset taken place following the formation of the protostar and heating up of the environment and the disk?

Planetary systems. Once the disk is dispersed (after ∼1-10 million years; Mamajek 2009), through a combination of accretion and (photoevaporative) winds (Alexander et al. 2006a,b; Ercolano & Pascucci 2017; Pascucci et al. 2023), the final stage of star- and planet-formation is marked by a remnant planetary system (see panel e of Figure 1), consisting of planets and larger planetesimals. These systems can still evolve due to interactions and collisions between the different bodies (see, for example, Wyatt 2018) and the evolution of the star itself.

1.2 Planet-forming disks

1.2.1 Disk constituents

Planet-forming disks consist of dust grains, gaseous molecules, and icy mantles coating the dust grains. Each of these constituents has its own distinct signatures, yet all three are inherently connected through both physical and chemical processes. Figure 1.2 displays a schematic overview of a planet-forming disk, highlighting key processes and observable signatures.

1.2.1.1 Dust and ice

Following their parent clouds, planet-forming disks consist of only a small percentage (∼1% by mass) of solid dust particles. These particles range from small micron-sized particles, which are well coupled to the gas particles, to larger millimetre-sized grains that have settled to the midplane and even larger, kilometre-sized planetesimals. Since the solid particles set the initial composition of rocky terrestrial planets and the cores of giant planets, understanding their chemical makeup is of great importance.

A dust grain itself is mainly composed of silicate material (Colangeli et al. 2003; Henning 2010). Throughout the ISM, the silicates are mainly amorphous

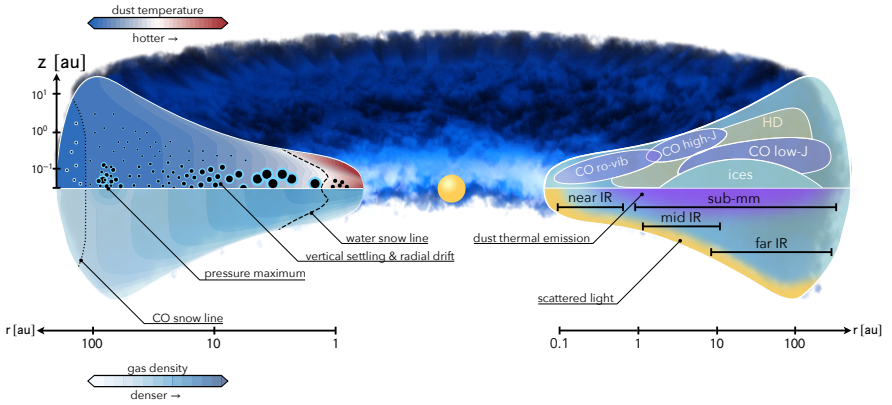

Figure 1.2: Schematic overview of a planet-forming disk. The left side of the image indicates the changing temperature (top) and density (bottom) structures across the disk. The right side of the cartoon displays the expected emitting regions of simple molecules (top) and the emitting wavelength range of different parts of the disk (bottom). This figure has been adopted from Miotello et al. (2023).

(i.e., the atoms are distributed in a disordered, random structure), whereas the presence of crystalline silicates (i.e., the atoms are distributed in an ordered, repeating structure) has been confirmed in disks (see, for example, Waelkens et al. 1996; Bouwman et al. 2001; Juhász et al. 2010). Crystalline silicates yield crucial information on the thermal history of the dust, as their formation may follow from either gas-phase condensation or thermal annealing of the amorphous grains (see, for example, Fabian et al. 2000). Infrared spectroscopy is of crucial importance for inferring the composition of the solid particles. Previous observations of the Infrared Space Observatory (ISO) and the *Spitzer* Space Telescopes (see, also, Malfait et al. 1998; Olofsson et al. 2009; Watson et al. 2009) and, more recently, JWST (Jang et al. 2024), have revealed that disks contain features of olivine ($Mg_{2x}Fe_{2-2x}SiO_4$, where $0 \leq x \leq 1$), pyroxene ($Mg_xFe_{1-x}SiO_3$, where $0 \leq x \leq 1$), forsterite (Mg_2SiO_4), and enstatite ($MgSiO_3$).

If a dust grain finds itself beyond the snowline - the boundary region in the disks where a molecule is for 50% in the gas and is for 50% frozen-out on the dust grains - it will be coated by an icy mantle. In reality, the snowline is a 2D structure, often referred to as a snow surface, following the temperature distribution in the disks, which decreases vertically downwards and radially outwards (see Figure 1.2). Since molecules have different binding energies, $E_{\rm bind}$, molecules with lower binding energies, i.e. apolar ices, such as CO and N_2 ($E_{\rm bind} \lesssim$1000 K; Bisschop et al. 2006), will freeze out at lower temperatures compared to those with higher binding energies (Boogert et al. 2015), i.e. polar ices, such as H_2O and CH_3OH ($E_{\rm bind} \gtrsim$5600 K; Penteado et al. 2017).

Similar to the dust grains themselves, direct observations of the ices yield information on the thermal history of an astronomical body. Heating can crystallise the ices, but also cause segregation - the separation of mixed ices - which yield unique ice features, such as the double-peaked CO_2 ice-band at 15 μm (Ehrenfreund et al. 1997; Gerakines et al. 1999; Pontoppidan et al. 2008b). Furthermore, infrared spectroscopy plays an important role in directly observing and disentangling the composition of the ices. However, the analysis of ice observations in planet-forming disks is not as straightforward. Due to scattering, a photon may have traversed different regions of a disk with different optical depths and, therefore, the observations need to be modelled in great detail (Sturm et al. 2023c,b,a).

1.2.1.2 Gas

Planet-forming disks are thought to be mainly comprised of gas, with a general mass fraction of ∼99%. The bulk of the gas is molecular hydrogen (H_2); however, the lack of a permanent dipole makes it hard to observe. With the first rotational excited state having a high upper level energy of $E_{\rm up}$ >500 K, the emission will be faint in the cold outer regions of the disk. The concepts of energy levels and transitions are explained in Section 1.3.1. Ro-vibrational transitions of H_2 with JWST now yield information on the hot, inner regions of the disks or extended emission that traces, for example, a wind/outflow. Therefore, other molecular species are needed to infer information on the bulk of the gas residing in disks. One such molecule is hydrogen deuteride (HD), of which only a few observations exist and the currently operating telescopes and instruments are not sensitive to its emission. Observations of the *Herschel* Space Observatory have allowed the detection of HD in the disks of TW Hydrae (Bergin et al. 2013), DM Aurigae, and GM Aurigae (McClure et al. 2016). Even though the interpretation of the observations is not without caveats and requires detailed modelling (Trapman et al. 2017; Kama et al. 2020; Calahan et al. 2021), the observations have allowed for constraints on the gas masses of these disks. Observations with the future space-based mission PRobe far-Infrared Mission for Astrophysics (PRIMA; Glenn et al. 2025), or the balloon-mission Planetary Origins and Evolution Multispectral Monochromator (POEMM; Stacey & POEMM Science Team 2025), may lead to more detections of HD in disks.

Carbon monoxide (CO), on the other hand, is a molecule that can be readily observed in disks. With an upper level energy of $E_{\rm up}$ ∼5 K, the fundamental J=1-0 rotational transition is a prime target for observations with, for example, ALMA. However, CO cannot be directly used as a proxy to estimate the total number of H_2 molecules and, therefore, the gas mass. This is mainly due to optical depth effects and uncertainties in the fractional abundance of CO with respect to H_2. Studies have shown that the fractional abundance can decrease from a value of $\sim10^{-4}$ to a value of 10^{-5} or 10^{-6} (see, for example, Zhang et al. 2021). Unless the fractional abundance is precisely known for a disk, the estimated mass may be off by a (few) order(s) of magnitude. Nonetheless, CO plays a crucial role in the analysis of planet-forming disks. Multiple studies have shown that observations of CO can be used to trace the disk's temperature structure (Law et al. 2021;

Leemker et al. 2022), to investigate its vertical extent (see, for example, Law et al. 2021; Paneque-Carreño et al. 2023), as well may be used to search for kinematical signatures from hidden planetary candidates (Perez et al. 2015; Pinte et al. 2019; Izquierdo et al. 2022).

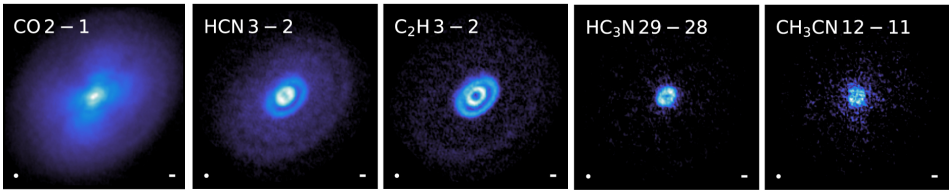

Figure 1.3: Various molecular species observed in the disk of HD 163296 with ALMA. This figure has been adapted from Öberg et al. (2021).

Aside from CO, a wide variety of other molecular species, both simple and complex, have been observed in planet-forming disks. Observations with ALMA have revealed that many molecular species, tracing different chemical processes, can be detected in the colder outer regions (see Figure 1.3). For example, ethynyl radical (C_2H), cyanide radical (CN), and hydrogen cyanide (HCN) have all been related to UV-driven chemistry (Jansen et al. 1995; Sternberg & Dalgarno 1995), while C_2H is also a direct tracer of the important elemental carbon-to-oxygen ratio (C/O-ratio) tracer (Bergin et al. 2016; Kama et al. 2016; Miotello et al. 2019). Similarly, the ratio of carbon monosulfide (CS) and sulfur monoxide (SO) can also be taken as a proxy for the C/O-ratio (Le Gal et al. 2021). SO, together with sulfur dioxide (SO_2) and other species, is also thought to be a tracer of (weak) shocks (see, for example, van Gelder et al. 2021; Booth et al. 2023). The molecular ions of formylium (HCO^+) and diazenylium (N_2H^+) are direct tracers of ionisation in the disk (Kastner et al. 1997; Öberg et al. 2011; Cleeves et al. 2015). HCO^+ can also be a direct tracer of X-ray flares from the host star (Waggoner & Cleeves 2022). N_2H^+, on the other hand, can directly trace the freeze-out and chemical transformation of CO (Qi et al. 2013; van 't Hoff et al. 2017), since its gas-phase formation is most efficient in the regions of the disk where CO is depleted and, therefore, may play a crucial role in determining the disk's gas mass (Trapman et al. 2022b). Deuterated formylium (DCO^+) and formaldehyde (H_2CO) are thought to trace cold chemistry (Öberg et al. 2010), since DCO^+ - similar to N_2H^+ - forms most efficiently in the gas around the CO snowline. H_2CO, on the other hand, can form efficiently in the gas (Fockenberg & Preses 2002; Atkinson et al. 2006), but it can also form efficiently on the icy dust grains through the hydrogenation of CO (Watanabe & Kouchi 2002; Fuchs et al. 2009; Santos et al. 2022). Upon further hydrogenation of H_2CO on the grains, methanol (CH_3OH), the simplest complex organic molecule (COM, a molecule with at least six atoms of which at least one is carbon; Herbst & van Dishoeck 2009) may form. Thus far, CH_3OH and other COMs, such as methyl formate (CH_3OCHO) and dimethyl ether (CH_3OCH_3), have mainly been found in the disks around young Herbig stars (van der Marel et al. 2021a; Brunken et al. 2022; Yamato et al. 2024a;

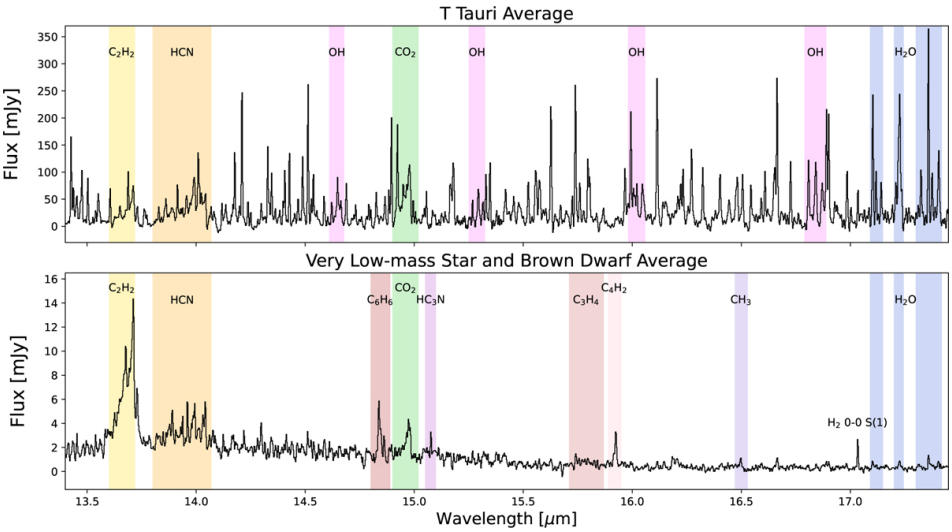

Figure 1.4: Averaged mid-infrared spectrum of a sample of T-Tauri disks (top) and VLMS disks (bottom). Detected molecular species are highlighted by the coloured areas. This figure has been adopted from Grant et al. (2025).

Booth et al. 2024a, 2025). As these disks are often too warm for CO to be directly frozen out, in situ formation of species like CH_3OH is unlikely, and the molecules are thought to be inherited from the earlier phases, as also evidenced by their association with icy dust traps.

Observations of *Spitzer* (Pontoppidan et al. 2010; Carr & Najita 2011) and, more recently, JWST reveal crucial information on the chemical composition of the hot, inner regions of planet-forming disks. In particular, the Medium Resolution Spectrometer (MRS; Wells et al. 2015) mode of the Mid-InfraRed Instrument (MIRI; Rieke et al. 2015) now provides the unique opportunity to study those inner regions with high sensitivity and resolution. The data reveal that the spectra of many T-Tauri disks are dominated by species like water (H_2O), hydroxyl radical (OH), carbon dioxide (CO_2), HCN, and acetylene (C_2H_2; see, for example, Grant et al. 2023b; Gasman et al. 2023; Temmink et al. 2024b,a, 2025b). This is in stark contrast to their lower-mass counterparts, as the spectra of VLMS disks are dominated by large hydrocarbons (Tabone et al. 2023; Arabhavi et al. 2024), such as ethylene (C_2H_4), ethane (C_2H_6), and even benzene (C_6H_6). The large contrast is displayed in Figure 1.4, where the average JWST spectra of a sample of T-Tauri disks and VLMS disks are presented (Grant et al. 2025).

1.2.2 Disk evolution

Planet-forming disks are not static objects, but they evolve. Crucial for the evolution of the disk is the distribution and conservation of angular momentum. Two leading hypotheses allow for the redistribution of angular momentum: viscous evolution (Shakura & Sunyaev 1973; Lynden-Bell & Pringle 1974) and magneto-

hydrodynamic (MHD) disk winds (Blandford & Payne 1982; Lesur et al. 2013). While both processes may be operating at the same time, it is thought that viscous evolution dominates during the early evolution of the disks, while MHD winds take over at a later stage (Trapman et al. 2022a). However, the main driver behind the evolution of planet-forming disks is still heavily debated (see, for example, Manara et al. 2023 and Pascucci et al. 2023). Other than the redistribution of angular momentum, processes such as accretion and accretion outbursts, planet formation and radial drift, and (photoevaporative) disk winds also play roles in the evolution of disks.

1.2.2.1 Viscous evolution

The viscous evolution model is based on the notion that the rotation velocity of a disk is not constant. Instead, according to Kepler's law, it decreases with the square of the radial distance with respect to the host star. Therefore, the inner regions of the disk rotate faster than the outer regions. If one considers two adjacent rings of gas, the one closer to the host star will rotate faster, and this creates a shearing force between the two bands. This friction causes angular momentum transfer between the two bands, where the inner band loses angular momentum and slows down, while the outer one gains angular momentum and speeds up. As a result, the inner band will move closer to the host star and may be accreted, while the outer band moves radially outward, effectively spreading the disk out over a larger distance (Shakura & Sunyaev 1973; Lynden-Bell & Pringle 1974; Pringle 1981).

The efficiency of this viscous spreading is set by the viscosity of the disk itself, which can be parametrised as (Shakura & Sunyaev 1973),

$$\nu = \alpha c_{\rm s} H. \tag{1.1}$$

Here, $c_{\rm s}$ is the sound speed, while H denotes the scale height of the disk. α is the dimensionless viscosity parameter whose value is heavily debated. While it was generally thought that a high viscosity value of α=10^{-2} is needed to explain the observations (Hartmann et al. 1998; Armitage 2015), more recent works suggest that a lower value of α $\sim$$10^{-3}$-$10^{-4}$ is more consistent with observations (see, for example, Flaherty et al. 2015; Trapman et al. 2020).

1.2.2.2 MHD disk wind

While the viscous evolution model suggests that the disk's radius increases with time, the MHD disk wind model suggests, instead, that the disk shrinks with time. The model relies on gas in the inner regions to be ionised, such that the gas, together with a large amount of angular momentum, can be removed through a disk wind following interactions with the magnetic field of the disk (see Lesur et al. 2023 for a recent review). Upon removal of the angular momentum, various modelling works have shown that this can yield efficient accretion onto the host star (Béthune et al. 2017; Zhu & Stone 2018; Tabone et al. 2022).

1.2.2.3 Accretion, accretion outbursts, and (late) infall

Both the viscous disk model and the MHD disk wind model show that accretion of disk material by the host star is inherent to the evolution of a disk. The accretion rate is not constant over the disk lifetime and can be paired with short-lived accretion (out)bursts that last a few hours or extreme events that last up to decades, but are much rarer (see Fischer et al. 2023 for a recent review). Both events can change the chemical composition of the disk over time, with the extreme events likely having a longer-lasting effect.

The short-lived events can be subdivided into three categories (Fischer et al. 2023): Routine Variability, Burst, and Outburst. During the first two events, the brightness of the star increases by a few magnitudes (up to a factor 10) and these last for a few hours to a week, whereas during an Outburst the brightness increases by several magnitudes (factors of >10) and lasts from months up to decades. As the brightness increases, the disk heats up, and this directly impacts the chemistry. As a result, snowlines are pushed further outwards, and molecules may sublimate - undergo a phase transition from solid to gas - from the icy grains. Smith et al. (2025) showed that the outbursting history of the system of EX Lup (Aspin et al. 2010) has pushed the H_2O snowline further out and increased the abundance of H_2O in the inner regions of the disk near the snowline. It is further expected that even Routine Variability can have this effect, where the snowlines are regularly pushed further out, and the emission can (temporarily) be enhanced due to sublimation.

A more extreme case is the system of V883 Ori, which underwent an extreme outbursting event that increased its luminosity to approximately $\sim$1000 $L_\odot$ (Leemker et al. 2021). This outburst has revealed the emission of H_2O and its isotopologues (HDO and D_2O) in the cold outer regions ($\sim$80 au) of the disk (Tobin et al. 2023; Leemker et al. 2025). The observations show that the isotope ratios, HDO/H_2O and D_2O/H_2O, are consistent with those found for the earlier protostellar phases and in comets of the Solar System. This suggests that the H_2O-ice in the cold outer disks is inherited from the earlier phases and that disks, therefore, play a crucial role in linking the chemical content of a planetary system with that of the ISM (Visser et al. 2009; Tobin et al. 2023). While H_2O plays a crucial role in linking the composition of ices across the different phases, the gas-phase reservoirs of other species, such as H_2CO, CH_3OH, and other COMs, are also enhanced by sublimation following an accretion outburst (see, for example, van 't Hoff et al. 2018; Lee et al. 2019; Yamato et al. 2024b; Calahan et al. 2024).

While accretion is often considered with respect to the host star, the disk itself may still accrete material from the immediate environment or the remnant envelope. In particular, streamers or late infalling material may replenish the disk with fresh material that can have a (local) effect on the chemical composition or (weakly) shock the disk, liberating ices from the grains (see, for example, Garufi et al. 2022). Existing observations reveal large-scale structures, extending up to thousands of au, in the disks of, for example, GM Aur (Huang et al. 2021) and SU Aur (Akiyama et al. 2019), in which the infalling material of SU Aur can even be traced by small dust grains (see Figure 1.5; Ginski et al. 2021).

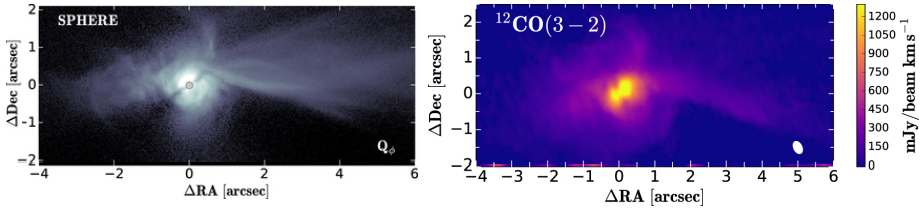

Figure 1.5: Late infalling material in the disk of SU Aur. The left image shows the extended visible in the small dust grains, while the right image displays those seen in the CO gas emission. This figure has been adapted from Ginski et al. (2021).

1.2.2.4 (Photoevaporative) disk winds

As opposed to accretion processes, where the disk gains mass, it may also lose mass through (photoevaporative) disk winds. One type of disk wind has previously been discussed, the MHD disk wind (see Section 1.2.2.2). The other type of wind that drastically changes the evolution of the disk in its later and may even lead to its dispersal is a photoevaporative (PE) wind (see Pascucci et al. 2023 for a recent review). Opposed to MHD winds, PE winds are thermally driven by EUV, FUV or X-ray radiation and do not affect the angular momentum transport within disks. A PE wind consists of gas that is heated up enough by the radiation such that its thermal energy exceeds the gravitational field of the host star.

Slow disk winds launched from the inner regions of disks, either driven by MHD or photoevaporation, can also be observed. Such winds have been proposed to explain the single-peaked line profiles of ro-vibrational CO observations (see, for example, Bast et al. 2011; Pontoppidan et al. 2011; Brown et al. 2013; Banzatti et al. 2022), although the precise origins of these winds are still under discussion. JWST observations of extended H_2 now also reveal the spatially resolved emission of disk winds (Arulanantham et al. 2024; Schwarz et al. 2025), also in the earlier Class I phase (e.g., Tychoniec et al. 2024).

1.2.2.5 Planet formation and radial drift

Even though planet formation is expected to already start in the earlier stages of star formation (Harsono et al. 2018; Tychoniec et al. 2020), the detection of protoplanets in the systems of PDS 70 (Keppler et al. 2018; Müller et al. 2018; Haffert et al. 2019) and WISPIT 2 (van Capelleveen et al. 2025) reveal that they directly impact the evolution of disks.

Planet formation follows from the evolution and coagulation of the dust grains (see Drążkowska et al. 2023 for a recent review). The evolution or growth of dust grains is the result of direct interactions with the gas particles. Because small (micron-sized) dust grains are coupled to the gas, they are located throughout the entire disk. Collisions between and efficient sticking of individual dust grains allow them to grow to millimetre-sizes (see, for example, Blum & Wurm 2008; Brauer et al. 2008; Birnstiel et al. 2010). Upon growing in size, the dust grains decouple from the gas. Gravitational effects cause the dust grains to settle to the

midplane, but the growth itself may be impeded as bouncing and fragmentation effects become important (Dubrulle et al. 1995; Duchêne et al. 2003; Villenave et al. 2020). An additional effect that impedes the growth of dust grains is radial drift. As the dust grains are decoupled from the gas, they move on Keplerian orbits, whereas the gas particles orbit with sub-Keplerian velocities. This velocity difference causes the dust grains to feel an aerodynamic drag force that causes the grains to lose angular momentum and move radially inward towards the host star.

Due to the radial decrease of temperature and density (see Figure 1.2), the disk has a negative pressure gradient (Drążkowska et al. 2023). With particles tending to move rapidly towards the host star, so-called pressure traps (localised pressure maxima; Pinilla et al. 2012b,a) may help overcome the growth barrier imposed by radial drift. Such pressure traps may be caused by embedded (planetary and (sub)stellar) companions in the disk (Pinilla et al. 2012a), hydrodynamical processes (such as the Rossby wave instability (RWI) and the vertical shear instability (VSI); Urpin & Brandenburg 1998; Lovelace et al. 1999; Li et al. 2000) and gravitational instability (Rice et al. 2004), and magnetohydrodynamic processes (such as zonal flows and dead zones; Gammie 1996; Hawley 2001; Johansen et al. 2009). Bae et al. (2023) contains a recent review on all these processes and their inner workings, which are beyond the scope of this thesis. As these pressure traps effectively create a pile-up of dust particles, the dust-to-gas ratio will locally increase, and this yields a favourable location of planetesimal formation, for example, through the streaming instability (Youdin & Goodman 2005; Drążkowska et al. 2016).

Aside from dust traps, snowlines - and, in particular, the H_2O snowline - may also yield favourable conditions for planetesimal formation. A pile-up of material near the snowline can also be caused by the cold-finger effect (Cuzzi & Zahnle 2004), where gaseous H_2O molecules inside the snowline are diffused radially outwards beyond the snowline and freeze out on the dust grains (Stevenson & Lunine 1988).

As soon as planetesimals have formed, the formation of planets may continue through one of two paradigms: planetesimal accretion or pebble accretion, see Drążkowska et al. (2023) for a recent review on both scenarios. Planetesimal accretion relies on the assumption that all bodies are planetesimals (sizes of $\gtrsim$10 kilometre) and that only the gravitational interactions between these bodies matter (Wetherill & Stewart 1989; Lissauer 1993; Kokubo & Ida 1996). As opposed to planetesimal accretion, pebble accretion is the addition of small dust grains to an already present larger body or planetary embryo (Johansen & Lacerda 2010; Ormel & Klahr 2010; Johansen & Lambrechts 2017). Additional differences between the two paradigms are their effective radial distances. Whereas planetesimal accretion only works in the immediate environment of the planetesimal, pebble accretion works over a larger area following the inward drift of the smaller pebbles (Ormel & Klahr 2010; Lambrechts & Johansen 2012). Furthermore, the efficiency of pebble drift depends on the mass of the planetary embryo and requires a large pebble reservoir (Guillot et al. 2014). As soon as the embryo hits the so-called pebble isolation mass - the mass where an embryo can open a gap in the disk and, as a result, a pressure maximum is generated exterior to the gap - pebble accretion

is halted (Lambrechts et al. 2014; Bitsch et al. 2018; Ataiee et al. 2018). The efficiency of planetesimal accretion, however, depends on the density of planetesimals in the region, and the efficiency of planetesimal accretion drops off quickly with the mass of the forming planet (see, for example, Kokubo & Ida 2002).

Once the planetary embryo is massive enough, either through planetesimal or pebble accretion, it may accrete gas from the surrounding disk, forming an atmosphere (or envelope) (Ikoma & Kobayashi 2025). With increasing mass of the embryo, the efficiency of gas accretion grows as well. If the mass of the embryo exceeds the critical mass - the mass where the total solid mass and envelope mass become equal - gas accretion continues through a runaway process and a gas giant planet forms (see, for example, Pollack et al. 1996). If the embryo never meets the critical mass, the resulting planets are more terrestrial-like and are dominated by solid material with a tiny atmosphere.

1.2.3 Disk observations

Due to both the dust constituents (dust and gas) and the changing thermal and density structure, observations at different wavelengths are sensitive to different components and regions of the disk (see the right side of Figure 1.2). Figure 1.6 shows an example of different types of observations for the disk of TW Hya (Andrews 2020), displaying the variations in morphology and radial extent of the small micrometre-sized dust grains, the millimetre-sized dust grains, and the CO gas emission. Observations spanning the near-infrared, mid-infrared, far-infrared, and (sub)-millimetre wavelengths are of particular interest for this thesis.

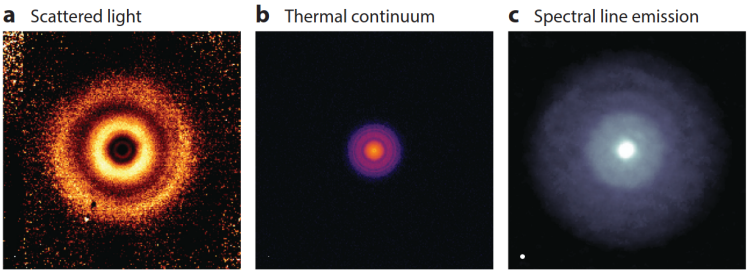

Figure 1.6: Different faces of the disk around TW Hya. The left panel shows the scattered light from the micrometre-sized dust grains, while the middle panel shows the thermal continuum emitted by the millimetre-sized dust grains. The right-most panel displays the extent of the gas disk. This figure has been adopted from Andrews (2020).

1.2.3.1 Near-infrared

Observations at wavelengths probing the near-infrared (NIR, $\lambda \sim$1-2.5 μm) regime trace the inner-most regions of planet-forming disks ($\lesssim$1 au). Furthermore, the NIR wavelengths are sensitive to the light scattered by the small dust grains at the disk's surface layer (see left panel of Figure 1.6) and, therefore, also provide

insights into the distribution of these small dust grains throughout the disk. While scattered light observations are not the focus of this thesis (see Benisty et al. 2023 for a recent review on the observations and techniques), they reveal key information on a disk's structure and configuration, which are highlighted in Section 1.2.4.

1.2.3.2 Mid-infrared

The IR wavelength regime is subdivided into different bands, of which the *L*- ($\lambda \sim$3.5 μm; Glass 1999) and *M*-band ($\lambda \sim$4.5 μm; Glass 1999) are most interesting for tracing the chemical conditions in a disk. With high spectral resolution, spectroscopic instruments on ground-based observatories like the CRyogenic high-resolution InfraRed Echelle Spectrograph (CRIRES, $R \sim$80,000; Kaeufl et al. 2004; Dorn et al. 2014, 2023) on the Very Large Telescope (VLT), iSHELL ($R \sim$80,000; Rayner et al. 2016, 2022) on NASA's Infrared Telescope Facility (NASA-IRTF), and NIRSPEC on Keck II ($R \sim$25,000; McLean et al. 1998), yield observations of ro-vibrational transitions of molecular species, such as CO, OH, H_2O, CO_2, HCN, methane (CH_4), and, C_2H_2 (see, for example, Mandell et al. 2012). In the not-too-distant future, the Mid-infrared ELT Imager and Spectrograph (METIS) on the Extremely Large Telescope (ELT) will yield additional observations of these regions and molecules with unprecedented sensitivity and resolution ($R \sim$100,000; Brandl et al. 2021).

While *L*- and *M*-band observations can be carried out from the ground, larger wavelengths need to be observed from space due to the Earth's atmosphere being opaque, mainly due to H_2O vapour, at these wavelengths. Space-based MIR observations have a rich history due to the wealth of information that was gathered with the ISO (1995-1998; Kessler et al. 1996) and the *Spitzer* Space Telescope (2003-2020; Werner et al. 2004). Recently, mid-infrared observations and, in particular, mid-infrared spectroscopy have been reinvigorated with the launch of JWST. With improved sensitivity, spatial resolution and spectral resolution ($R >$1500-3000 compared to *Spitzer*'s $R \sim$90; Houck et al. 2004), JWST's MIRI instrument is crucial in revealing the chemical composition of the inner ($\leq$10 au) of planet-forming disks (see Figure 1.4). Chapters 2, 3, and 4 of this thesis make use of JWST-MIRI observations as part of the Guarranteed Time Observations (GTO) Miri Mid-Infrared Disk Survey (MINDS, PI: T. Henning; Kamp et al. 2023; Henning et al. 2024) collaboration. As discussed in Section 1.2.1.2, these observations cover transitions of H_2O, CO_2, HCN, C_2H_2, and more. Additionally, the Near-InfraRed Spectrographa (NIRSpec; Jakobsen et al. 2022) instrument onboard JWST can be used to cover molecular transitions in the 2.5-5 μm wavelength range, although many nearby planet-forming disks exceed its brightness limit and saturate the detector.

1.2.3.3 Far-infrared and (sub-)millimetre

At even longer wavelengths, instruments observing in the far-infrared (FIR) and (sub-)millimetre regimes probe the outer regions of planet-forming disks ($\gtrsim$10 au). Since the decommissioning of the *Herschel* Space Telescope (2009-2013; Pilbratt et al. 2010), now over a decade ago, no telescope or instrument probing the FIR

wavelength regime exists. However, this may change with the proposed observatories of PRIMA and POEMM.

While there is a lack of FIR instruments, (sub-)millimetre astronomy is thriving. Not only due to the high sensitivity and resolution of ALMA, but also that of the Northern Extended Millimeter Array (NOEMA) and the Submillimeter Array (SMA; Ho et al. 2004). The power of (sub-)millimetre astronomy can be found in the use of interferometric techniques offering much higher spatial resolution. By combining the observations of multiple individual antennas, the dust and gas in planet-forming disks can be spatially resolved, yielding unique insights into their distributions and structures. ALMA has a total of 66 antennas (50 12-metre in an extended configuration and 4 12-metre and 12 7-metre antennas in a compact configuration) that form effective telescope diameters from 150 metres to a total of 16 kilometres. As the ALMA antennas have different receiver bands, the maximum achievable spatial resolution depends on the observing wavelength and the maximum baseline between the different antennas. In the most extended configuration in ALMA Band 10 (0.3-0.4 millimetre or frequencies of 787-950 GHz), ALMA can reach spatial resolution down to 5 milliarcseconds (0.005"). For a planet-forming disk at 140 parsecs (see, for example, Kenyon et al. 1994), the approximate distance to the Taurus star-forming region, this allows details to be discernible at scales of 0.7 au, corresponding to the orbit of Venus. However, at these short wavelengths (or high frequencies), the Earth's atmosphere nearly becomes opaque to (sub-)millimetre radiation and, therefore, low atmospheric water vapour levels are required for successful observations. Aside from high spatial resolution capabilities, ALMA also allows for high spectral resolution observations. With a maximum resolution of 0.01 km s^{-1} (or 10 m s^{-1}), the dynamics of the gas can be studied in great detail.

1.2.4 Disk substructures

The first high spatial resolution image of a planet-forming disk taken by ALMA revolutionised our vision of these systems. The image revealed that the dust disk around the young star HL Tau was not smooth but consisted of multiple rings and gaps (ALMA Partnership et al. 2015). With ALMA, many of these substructes have been found, ranging from these gapped disks to disks with large cavities and even asymmetric features (van der Marel et al. 2013; Casassus et al. 2013). While substructures in the millimetre dust continuum generally gain the most attention, similar structures can also be found in the scattered light and gas emission (see Andrews 2020; Bae et al. 2023; Benisty et al. 2023 for recent reviews). Crucially, a disk can contain multiple types of substructures, and the structures do not have to match between the different types of observations (i.e., a disk can physically look different in the millimetre continuum emission and scattered light; see, for example, Figure 1.6).

1.2.4.1 Rings and gaps

The type of substructure that is most commonly found is that of rings and gaps, similar to the disk of HL Tau. The system of HL Tau is rather unique, given its high multiplicity of rings (a total of 7 have been identified; ALMA Partnership et al. 2015). While multi-ring systems are not uncommon, a large sample of disks only seems to contain a single ring. It must be noted, however, that the majority of disks have not been observed with the highest spatial resolution and, therefore, rings and other substructures may currently be hidden from our view.

One of the leading theories for the formation of (multiple) rings and gaps are (planetary) companions embedded in the disks. In this scenario, the companion directly carves a gap in the disk (i.e., accreting all the dust grains on their orbit), which yields a pressure bump at the outer boundary of the gap (Pinilla et al. 2012b,a). The properties of the gap (that is, its width and depth) depend on the mass of the companion, in addition to the viscosity of the disk and temperature (see van der Marel & Pinilla 2023 for a recent view). It is, however, not well understood whether the number of observed gaps directly translates to the number of (planetary) companions in the system. It has been shown, for example, that a companion can open multiple gaps due to migration (Bae et al. 2017; Dong et al. 2017; Wafflard-Fernandez & Baruteau 2020).

1.2.4.2 Rings and cavities

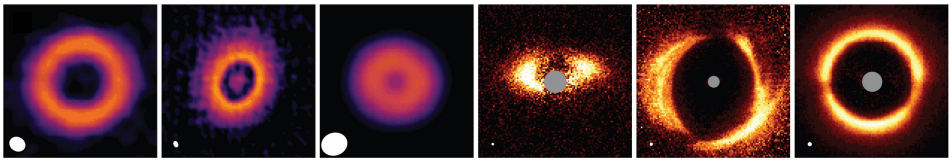

Figure 1.7: Disks with large inner cavities. The first three images are of the millimetre dust continuum, whereas the latter three are taken in scattered light. From left to right: RXJ1604.3-2130, DM Tau, DoAr 44, Oph-IRS 48, HD 142527, and RXJ1604.3-2130. This figure has been adapted from Andrews (2020).

Aside from multiple rings and gaps, depleted cavities are also commonly observed substructures (see Figure 1.7). Such systems, which lack strong dust emission from their inner regions, are known as so-called transition disks (Espaillat et al. 2014; van der Marel 2023) and were originally identified through their spectral energy distributions (SEDs; Strom et al. 1989; Skrutskie et al. 1990). Their SEDs lack an excess of NIR and MIR emission, which are otherwise an indication of the presence dust grains in the inner region. Similar to the origins of rings and gaps, the most popular theory for the depleted cavities is (planetary) companions. A famous example is the PDS 70 system, where two known planetary companions can be found in the cavity (Keppler et al. 2018; Müller et al. 2018; Haffert et al. 2019). Other than companions, photoevaporative winds (Hollenbach et al. 1994; Alexander et al. 2006a,b; Espaillat et al. 2014) and the edges of dead zones may also yield large cavities (see, for example, Regály et al. 2012).

While these cavities are devoid of dust grains, gas may still be present. Gas inside the cavity was first indirectly inferred through signatures of accretion (Najita et al. 2007). In addition, detailed analysis of the CO ro-vibrational transitions showed that the cavity in the gas could be smaller than the one in the dust (Pontoppidan et al. 2008a; Brittain et al. 2009; Salyk et al. 2009). Spatially resolved images with ALMA now directly reveal the presence of gas inside the cavities (see, for example, Bruderer et al. 2014; Pérez et al. 2014; van der Marel et al. 2016b). Whether gas can be found in the cavity or not depends on its formation. If the cavity is due to a photoevaporative wind, it is expected that the cavity is fully depleted of both dust and gas. Similarly, a massive companion, such as a gas giant planet, carving a gap in the dust is expected to also carve a gap in the gas, the depth of which is again dependent on the companion's mass and the disk's viscosity. A dead zone, on the other hand, is not expected to result in a change in the gas surface density (van der Marel et al. 2016b).

1.2.4.3 Asymmetries

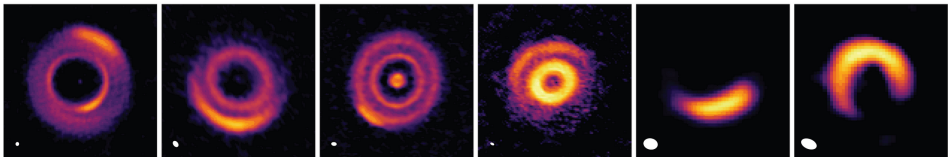

Figure 1.8: Disks with observed asymmetric features in the millimetre dust continuum. From left to right: MWC 758, HD 135344B, HD 143006, V1247 Ori, Oph-IRS 48, HD 142527. This figure has been adapted from Andrews (2020).

Asymmetric features, also described as arcs or crescents, are much rarer compared to rings, cavities and gaps (Andrews 2020; Bae et al. 2023). They can, however, be found in a variety of scenarios. The most extreme of which is a partial ring, an arc-like structure, around a cavity. Additional asymmetries are arc-like structures in ringed systems (Marino et al. 2015a; van der Marel et al. 2016a; Kraus et al. 2017) or arc-like structures inside a cavity (Isella et al. 2018; Long et al. 2022). Figure 1.8 provides a few examples of planet-forming disks with asymmetries.

One of the leading theories for asymmetric features is vortices. Various hydrodynamic instabilities can lead to vortices, which include the RWI. In particular, an anticyclonic vortex is thought to have a pressure maximum at its centre (Lovelace & Romanova 2014), which effectively can trap the dust in these arc-like features. An anticyclonic vortex can decay after many orbits (Godon & Livio 1999; Rometsch et al. 2021), (re-)distributing the material in a ring-like morphology. The RWI can be generated by a (planetary) companion, at the inner edge of a dead zone, or by late infalling material (see Bae et al. 2023 for a recent review). The last scenario has recently gotten more observational traction with the suggestion that late infalling material may be the cause of the observed asymmetries in the disks of HD 34700A (Stadler et al. 2026) and HD 142527 (see Chapter 7 of this thesis).

The gas emission of an asymmetric disk is also of great interest. In particular, azimuthally asymmetric disks are thought to be a perfect laboratory for studying the direct connection between the dust and gas composition. The case the Oph-IRS 48 disk, the most asymmetric disk known to date (van der Marel et al. 2013), is a great example. The molecular emission of Oph-IRS 48 (second to last disk in Figure 1.8), which ranges from simple molecules (such as NO, SO and SO_2) to complex molecules (such as CH_3OH and CH_3OCH_3), is found to be more or less co-spatial with the millimetre continuum emission (Booth et al. 2021a, 2024b; van der Marel et al. 2021a; Brunken et al. 2022; Leemker et al. 2023). This suggests strongly that the dust trap is an ice trap and the molecular emission becomes visible due to sublimation of the ices following efficient radial and vertical transport of the icy dust grains to elevated layers near the inner edge of the dust trap. However, interpreting the data became more complex by the realisation that processes like photodissociation can efficiently destroy the molecules in these layers. Furthermore, the photodissociation products may actually be used in the gas-phase formation of different species, yielding distinct reservoirs of molecules that either sublimate from the grains or were formed directly in the gas (Temmink et al. 2025a; see Chapter 6 of this thesis).

Another example is the asymmetric disk of HD 142527 (Fujiwara et al. 2006; Ohashi 2008; Casassus et al. 2013; the last disk in Figure 1.8). As opposed to Oph-IRS 48, the gas emission in HD 142527 is not co-spatial with the dust trap. Instead, the emission peaks on the opposite side of the disk (van der Plas et al. 2014; Temmink et al. 2023). The discovery of spiral arms in the gas emission of CN, C_2H, and H_2CO, suggests that te molecular is unrelated to the dust, but are, instead, thought to be the result of late-infalling material (see Chapter 7 in this thesis).

1.2.4.4 Spiral arms

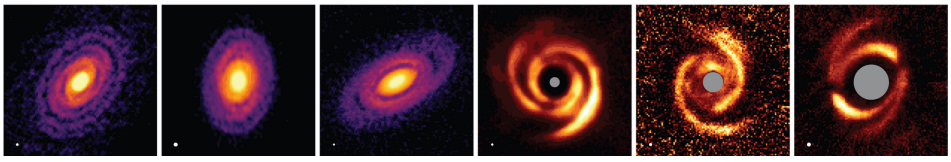

Figure 1.9: Disks with observed spiral arms. The first three images are of the millimetre dust continuum, whereas the latter three are taken in scattered light. From left to right: IM Lup, WaOph 6, Elias 27, HD 135344B, MWC 758, and HD 100453. This figure has been adapted from Andrews (2020).

Spiral arms are predominantly observed in the scattered light, in contrast to other substructures (see, Benisty et al. 2023, for a recent view). Only a handful of disks have confirmed detection of spiral arms in the millimetre continuum emission (see, for example, Huang et al. 2018a), but they are more common in the CO gas emission (Christiaens et al. 2014; Teague et al. 2019; Wölfer et al. 2023). Various explanations exist for the origin of spiral arms in planet-forming disks.

These range from density perturbation caused by embedded (planetary) companions (Kley 1999) or gravitational instability (Rice et al. 2004), to interactions with the surrounding material, such as a remnant cloud envelope or late infalling material (Lesur et al. 2015; Kuznetsova et al. 2022). Additionally, interactions (or fly-bys) between the stars of a wide-separation binary (Mayama et al. 2020; Ménard et al. 2020) and shadows (Montesinos et al. 2016; Zhang et al. 2025) may also launch spiral-like features in a disk.

Aside from seeing spiral arms in the CO gas emission, the role of spirals in setting the observable chemistry is not well known. One way spirals can affect the chemistry is through (weak) shocks. The detection of SO, a well known shock tracer, has been attributed to shocks induced by spirals arms in the disks of AB Aur (Speedie et al. 2025), CQ Tau, and MWC 758 (Zagaria et al. 2025). Recently, spiral-like features were seen in the emission of H_2CO, C_2H, and CN (see Chapter 7 of this thesis). These features are thought to be the result of infalling material that replenish the disk with fresh material and, therefore, allows for the gas-phase formation of these molecules.

1.2.4.5 Shadows and misalignments

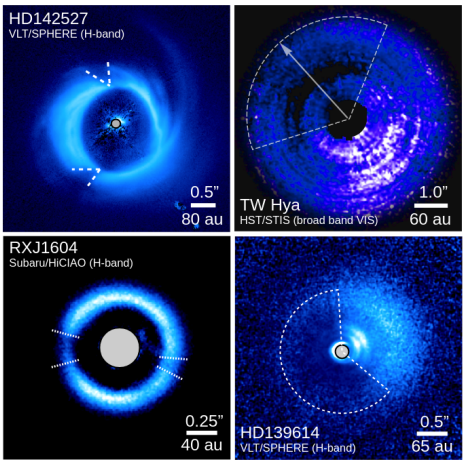

Figure 1.10: Shadows in the scattered light images of four disks. The left two disks have shadows confined to small azimuthal increments, whereas the right two disks show broad shadows. This figure has been adapted from Benisty et al. (2023).

Shadows are another feature that is predominantly observed in the scattered light. Shadows are dips in a disk's brightness profile at confined azimuthal angles (see Figure 1.10; Benisty et al. 2023). The observed shadows are divided into two categories: the first category contains disks with narrow shadows spanning small azimuthal increments, while the second category consists of disks with shadows spanning a wide azimuthal increment (up to half the disk's azimuthal extent).

The appearance of shadows is often linked with a misaligned inner disk, that

is, the inner disk is inclined with respect to the planet of the outer disk. The misalignment causes part of the starlight to be blocked, effectively casting a shadow at the outer regions (Marino et al. 2015b). A larger misalignment is thought to yield the narrow shadows, while a smaller misalignment will yield the broader shadows. The misalignment is often considered to be the result of a dynamical perturbation by a close-in companion. For a handful of disks, this theory of a misaligned inner disk has been confirmed to be the cause of the shadows (Benisty et al. 2018; Bohn et al. 2022).

Other than dynamical perturbations, shadows may also be caused by interactions with late infalling material (SU Aur; Ginski et al. 2021) or material surrounding a binary system, such as is the case for GG Tau A (Krist et al. 2002; Itoh et al. 2014; Keppler et al. 2020). Additional explanations for shadows in disks without misalignments can be found in irregular or lifted dust clumps either through magnetospheric accretion or disk winds (Pinilla et al. 2018; Rich et al. 2019).

1.2.4.6 Substructures and radial drift

The observed substructures, especially those in the millimetre dust continuum, are thought to be mainly the result of pressure traps (see Section 1.2.2.5). These structures may, therefore, prevent radial drift and facilitate the formation of planetesimals and larger bodies (see, Birnstiel 2024, for a recent review). If radial drift is impeded by substructures, not only may this facilitate planet formation, but it may also impact the observable chemistry. Radial drift, after all, will bring ices from the outer regions into the inner parts of disks where they may sublimate and enrich the gas.

With many important snowlines (i.e., those of H_2O and CO_2) being located in the inner few au of the disks, close to the host star, the importance of radial drift and substructures has regained attention with the launch of JWST. In particular, Banzatti et al. (2020) proposed a simple scenario where the H_2O reservoir in the inner regions of small disks ($R_{\rm dust}$ $\leq$60 au) is enhanced due to efficient radial drift and subsequent sublimation of the H_2O-ice, whereas that in larger disks ($R_{\rm dust}$ >60 au) with structures is not enhanced as the drifting grains are trapped in the structures. For disks with large cavities, the H_2O reservoir was expected to be depleted. Recent works have now shown that this scenario is much more complex, as disks with large cavities can have H_2O in their inner regions (Perotti et al. 2023; Schwarz et al. 2024; Mallaney et al. 2026) and not every small disk is enhanced in the H_2O reservoir (Temmink et al. 2025b; see Chapter 4 of this thesis).

Models that can test the efficiency of gaps in stopping the drift, for example, by including gaps with different depths and widths, further complicate this story. It has been shown that the effect of H_2O-enhancement in the inner regions is only temporary, up to a few million years, when gaps are considered (Kalyaan et al. 2021, 2023). The enhancement can be prolonged if small grains are considered or if the gaps are less deep and, therefore, more susceptible (or leaky) to grains passing through (Pinilla et al. 2024; Mah et al. 2024). Additionally, the radial location of

the gap matters a lot (Kalyaan et al. 2023; Sellek et al. 2025). If a gap is located closer to the host star, the influence of a gap halting the drift will be greater than if the gap were located further out. Finally, models that study the effect of dust optical depth have also shown that the enhancement of the gas reservoirs following radial may not be visible at all, as drifting particles also enhance the dust density in the inner regions (Sellek et al. 2025; Houge et al. 2025).

The relation between substructures, radial drift, and the molecular composition, is, therefore, rather complex. From an observational point of view, many aspects require further study. For example, the models have shown that gaps located at closer radial distances are more important for impeding drift. Detecting structures at these distances requires high spatial resolution observations with, for example, ALMA, and special super-resolution techniques to hunt for substructures at smaller scales than can be resolved directly from the images (see, for example, Tazzari et al. 2016, 2017; Jennings et al. 2022a). Additionally, the efficiency of radial drift has not been studied for a large number of disks. Trapman et al. (2019) proposed a scenario where the ratio between the gas and dust disk sizes ($R_{\rm gas}/R_{\rm dust}$) can be used as an estimate for the efficiency of radial drift. If this ratio is larger than 4, the disk is expected to undergo very efficient radial drift, explaining the smaller size of the dust disk. A great example is the small disk of CX Tau, where Facchini et al. (2019) reported a value of $R_{\rm gas}/R_{\rm dust}$ >5. While observations of the gas and dust exist for a large number of disks, this ratio has not been estimated for many of them. The importance of radial drift and substructures on the observable chemistry can be further explored by continuing to hunt for substructures in disks (in particular, those at smaller radial distances) and combining this with the estimated ratios of the gas disk and dust disk sizes.

1.3 Astrochemistry

Astrochemistry is the field of study that combines astronomy and chemistry by studying (either through observations, theory, or experiments) the abundances of elements and ongoing chemical reactions in space (see Tielens 2013; van Dishoeck 2014 for recent reviews). Observationally, molecules can be directly studied in emission, where a photon is emitted following the energetic transition form a higher state to lower state. Conversely, molecules can also absorb light by undergoing such a transition from a lower to a higher state. Throughout the remainder of this chapter, we only focus on the emission of light.

1.3.1 Energy levels and transitions

Molecules have three distinct types of energy levels: electronic, vibrational, and rotational (Figure 1.11, see Tennyson 2019; Tielens 2021 for extensive overviews of energy levels and spectroscopy). The energy levels are structured, where a single electronic energy level is subdivided into various vibrational levels, and each vibrational level is subdivided into many rotational states. For levels closer together (i.e., rotational levels), less energy is required for a transition to happen compared

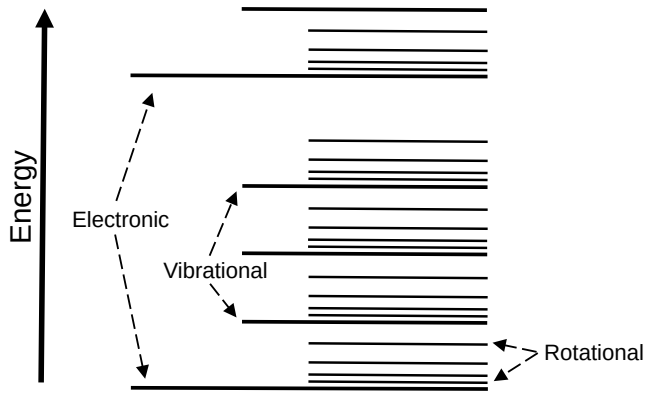

Figure 1.11: Schematic of the different energy levels.

to levels that are separated by a larger distance (i.e., vibrational and electronic levels). As the difference between energy levels (ΔE) is directly connected to the wavelength of a photon (λ), $\Delta E = hc/\lambda = h\nu$, the different levels emit or absorb at different wavelengths. The electronic transitions involve photons that emit at optical wavelengths, whereas those following from vibrational and rotational transitions emit at, respectively, infrared and (sub-)millimetre or radio wavelengths. In equation for the energy levels, h denotes the Planck constant, c the speed of light, and ν is the frequency of the light emitted by a photon. As electronic transitions are not part of this thesis, we focus on the vibrational and rotational transitions in the remainder of this section. In planet-forming disks, a molecule is generally collisionally excited from the ground (i.e., the state with the lowest energy) to a higher energetic state, where the collisional partner is mainly H_2, before it cascades back down to the ground state by emitting a photon.

1.3.1.1 Ro-vibrational transitions

During a transition between vibrational levels, the rotational level may also change, resulting in so-called ro-vibrational transitions. The change in a rotational level is denoted by the quantum number ΔJ, and can have values of ΔJ=0,$\pm$1. For linear molecules with a denegerate bending mode where all three values of ΔJ are allowed (such as CO_2, HCN, and C_2H_2), the ro-vibrational spectrum has a distinct layout: as vibrational transitions with no change in the rotational level have similar energy differences, photons with very similar wavelengths are emitted. This yields a very broad spectrum in the feature that is known as the Q-branch. If ΔJ=-1, the transition happens between energy states that are closer together in energy space and, therefore, ΔE is smaller. This, therefore, yields distinct transitions (also known as the P-branch) to the right of the Q-branch when plotted as a function of wavelength. Conversely, transitions with ΔJ=+1 yield distinct transitions (also known as the R-branch) to the left of the Q-branch. For diatomic molecules (such as CO), the Q-branch transitions are forbidden, yielding a spectrum consisting

of only the P- and R-branches. An asymmetric top molecule, such as H_2O, has a very irregular spectrum due to additional ortho and para states with different rotational levels. Simulated spectra of each of these molecules are displayed in Figure 1.12 to highlight the differences.

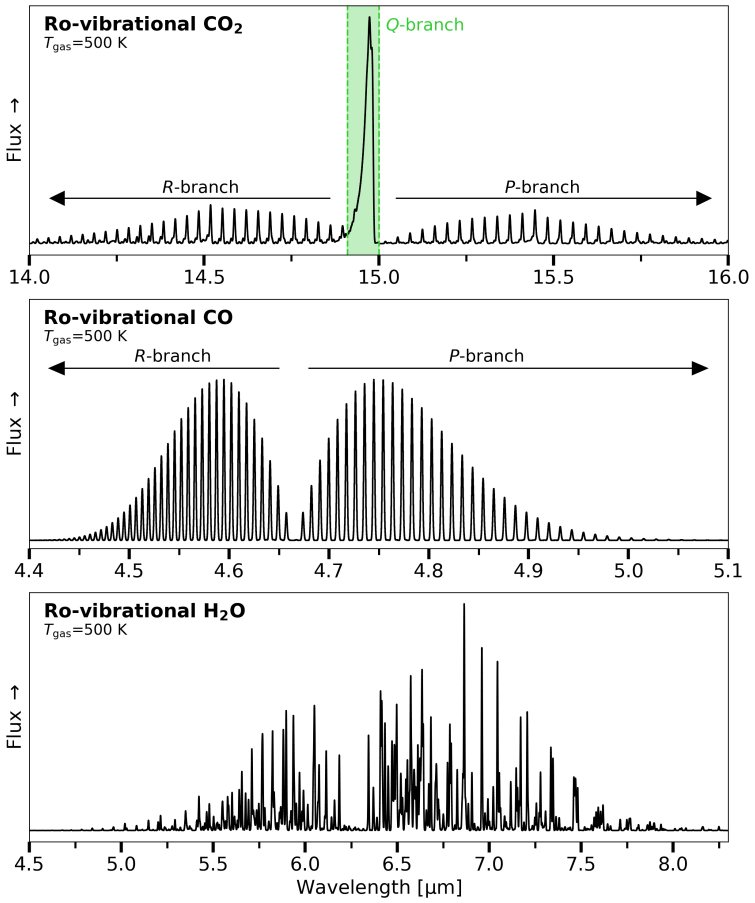

Figure 1.12: Simulated, optically thin ro-vibrational spectra of CO_2 (top panel), CO (middle panel), and H_2O (bottom panel) at $T_{\rm gas}$ =500 K. The Q-, P- and R-branches of CO_2 and the P- and R-branches of CO are indicated.

1.3.2 Excitation analysis

The spectra provide direct information on the properties of the gas. The intensity of each line is, after all, directly related to the column density of the molecular species ($I \propto N$). The ease of the analysis depends on whether the molecular excitation is in local thermal equilibrium (LTE) or not. In the case of LTE, the density of the gas is sufficiently high such that it exceeds the critical density, and

the level populations can be described by a single a excitation temperature ($T_{\rm ex}$), their distributions are proportional to $n_{\rm i} \propto \exp(-E_i/k_{\rm B}T_{\rm ex})$. Here, E_i is the upper level energy of the i-th transition.

One aspect that complicates an excitation analysis is the notion of optical depth. Optical depth (τ) is a measure of the transparency of a material to light. If the molecular gas is optically thin ($\tau \ll 1$), the emission of these species throughout the entirety of an astronomical object (i.e., a cloud or a disk) can be observed. However, once the emission becomes optically thick ($\tau \geq 1$), the emission will not be able to penetrate the optically thick gas, and only part of the molecular column can be observed. If the optical depth is known, a correction factor ($1 - \exp(-\tau)$) to the column density can be applied during an excitation analysis, but precise estimations of the optical depth are hard to obtain. Optically thick emission can, however, be extremely useful if one is interested in the temperature of a gaseous medium. In this case, the brightness temperature provides a direct estimate of the kinetic temperature ($T_{\rm kin}$) of the gas.

Furthermore, it is not only the optical depth of the gas that needs to be taken into account when inferring the column density of a molecular species. The optical depth of the dust, which is wavelength dependent, matters as well, especially at NIR and MIR wavelengths, as the smaller micrometre-sized dust grains are distributed throughout the entire disk. Once the dust becomes optically thick ($\tau_{\rm dust} \geq 1$) at a certain wavelength, it will absorb emission originating from deeper inside the disk.

In the case of non-LTE emission, the analysis of the molecular emission requires full radiative transfer calculations (see, for example, van der Tak et al. 2007) and extensive knowledge of the collisional rate coefficient of the molecule with a collisional partner (often H_2). An example is given by the sub-thermal excitation in the low-density regions of planet-forming disks, such as their surface layers. For CH_3OH, simulations at low densities ($n_{\rm gas} \sim 10^7$ cm^{-3}) found excitation temperature significantly below the kinetic tempreature of the gas (i.e., $T_{\rm ex} \neq T_{\rm kin}$; Johnstone et al. 2003). Upon increasing the density of the gas ($n_{\rm gas} \sim 10^9$ cm^{-3}), the excitation temperature nearly matched the kinetic temperature ($T_{\rm ex} \sim T_{\rm kin}$), implying that the emission had thermalised and, therefore, LTE could be assumed.

Aside from low-density environments, non-LTE excitation can also be due to IR or UV pumping and prompt emission following the formation of the molecule. Both of these processes can be very important for JWST observations. The emission of SO_2 at 7 μm in the protostar NGC 1333 IRAS 2A has been attributed to IR pumping (van Gelder et al. 2024), where the absorbance of IR photons leads to increased populations of higher energy levels than can be expected from collisional excitation alone (Bruderer et al. 2015; Bosman et al. 2017). Prompt emission occurs when a molecule ends up in a higher excited state following, for example, the photodissociation of its parent species (Tabone et al. 2021). For disks, this can be very important for the emission of OH, since it is the photodissociation product of H_2O (Carr & Najita 2014; Tabone et al. 2024).

1.3.3 Chemical processes

As described before, the important constituents of the stages of star- and planet formation (and, therefore, planet-forming disks) are the gas, the dust grains, and the icy mantles coating the grains. Important processes that regulate the observable chemistry are, therefore, subdivided into gas-phase reactions and processes occurring on the surfaces of grains or in the ices (see Figure 1.13). Öberg & Bergin (2021) and van't Hoff & Bergner (2026) contain recent reviews on the ongoing chemical processes in disks.

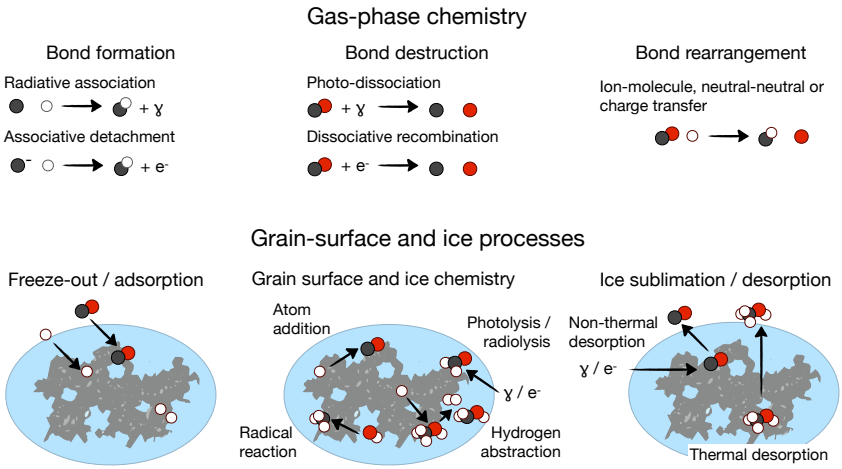

Figure 1.13: Overview of the ongoing chemical processes in the ISM and planet-forming disks. The gas-phase processes are shown on the top, whereas the bottom is dedicated to grain-surface and ice processes. This figure has been adapted from Öberg & Bergin (2021).

1.3.3.1 Gas-phase chemistry

The conditions (i.e., low densities and temperatures) in planet-forming disks are generally not suited for three-body reactions. Instead, the chemistry is driven by two-body reactions. These reactions involve bond formation (radiative association and associative detachment), bond destruction (photodissociation and dissociative recombination), and bond rearrangement (ion-molecule, neutral-neutral, and charge transfer) processes. Only within the innermost regions of disks, where the densities ($n_{\rm gas} \gtrsim 10^{12}$ cm^{-3}) and temperatures ($T >$100 K) are high, three-body processes may become important (see, for example, van't Hoff & Bergner 2026). As three-body processes are beyond the scope of this thesis, the remainder of this section focuses on two-body processes.

Bond formation. Out of the two gas-phase bond formation processes, radiative association is considered to be the most important. However, due to the radiative stabilisation of the molecule through vibrational transitions taking much

longer than collisional timescales, the likelihood of such reactions taking place is small. Therefore, radiative association is most efficient and important for reactions involving reactants that are very abundant, such as atomic and molecular hydrogen (H and H_2; Herbst & Klemperer 1973). Compared to radiative association, associative detachment is much rarer as the reactions involve anions (negatively charged ions, like OH^-; Millar et al. 2007).

Bond destruction. The destruction of a molecule through the absorption of a photon is known as photodissociation (see Heays et al. 2017 for an overview). While the majority of molecules are directly destroyed if the energy of the photon is higher than the covalent bond strengths, generally requiring ultraviolet (UV, or higher) energies, molecules like H_2 and CO dissociate through the absorbance of specific lines (that is at specific wavelengths or frequencies; Stecher & Williams 1967; Abgrall et al. 1992). The molecule is, in that case, in an excited state from which it can move into a dissociated state (also known as predissociation and works for CO; van Dishoeck & Black 1988) or dissociate through spontaneous decay (H_2). As the photodissociation of H_2 and CO involves specific lines, self-shielding effects can become very important in halting the destruction. Self-shielding occurs when the gas becomes optically thick against the incident radiation and, therefore, deeper layers are effectively shielded against photodissociation.

UV-photodissociation is inherently linked with photon-dominated regions (PDRs; Tielens & Hollenbach 1985), regions that are subject to immense UV-irradiation from nearby (massive) stars. A well-known example is the Orion Bar south of the Trapezium Cluster. The surface layers of planet-forming disks can, effectively, also be considered to be PDRs, as these regions are directly subject to irradiation from the host star (van Dishoeck 2006; Bergin et al. 2007). The structure of a PDR is simple: closest to the radiation source, the majority elements are in ionised atomic states (i.e., C^+). Deeper into the PDR (or disk surface layer), the atoms will be in a neutral state, and even deeper, the elements can be bound up in molecules.

Through collisions with electrons, ions may also be destroyed in favour of forming two neutral molecules or an atom and a molecule. As a result of dissociative recombination, both smaller (i.e., $HCO^+ + e^- \rightarrow HCO$; Herbst & Klemperer 1973) and larger molecules can form (i.e., $CH_3CNH^+ + e^- \rightarrow CH_3CN + H$; van't Hoff & Bergner 2026).

Bond rearrangement. Of the gas-phase bond rearrangement processes, ion-neutral reactions dominate the gas-phase chemistry in planet-forming disks. As ions are required for these processes, a source of ionisation is required. Within disks, ionisation occurs through UV irradiation, X-rays, cosmic rays, and radionuclides (Glassgold et al. 1997; Walsh et al. 2012; Eistrup et al. 2016). For ion-molecule reactions, H_3^+ plays a crucial role. H_3^+ forms after an ionisation event of H_2, and its density is found to be largely constant. Therefore, the gas-phase chemical timescale is largely influenced and set by H_3^+. Well-known examples are the formation of HCO^+ ($H_3^+ + CO \rightarrow HCO^+ + H_2$; Herbst & Klemperer 1973) and H_2D^+ ($H_3^+ + HD \rightarrow H_2D^+ + H_2$; Watson 1976), a molecule driving the deuteration of other species.

While neutral-neutral and charge transfer reactions are less dominant, they still

can play a crucial role in setting the abundance of certain species. An example of neutral-neutral reactions is related to the formation of H_2O and CO_2 through reactions with OH (respectively, H_2+OH $\rightarrow$ H_2O+H and CO+OH $\rightarrow$ CO_2+H; Charnley 1997; van Dishoeck et al. 2013; Bosman et al. 2022b). In the hot inner regions of disks (T >200 K) the gas-phase formation of H_2O dominates over the gas-phase formation of CO_2. In the colder regions (T <200 K), it is the formation of CO_2 that is more efficient.

1.3.3.2 Grain-surface chemistry

While grain-surface chemistry is not the direct focus of this thesis, ices are extremely important for the chemistry of planet-forming disks. Through freeze-out and sublimation processes, grains directly affect the observable chemistry by either depleting the molecular reservoir (freeze-out) or enhancing it (sublimation). Within disks, this is all regulated by snowlines. The release of a molecule from the grain inside its snowline following, for example, radial drift is known as a thermal desorption process, but various non-thermal processes also occur. These processes include photodesorption, chemical desorption, and shocks (see Cuppen et al. 2024 for a recent review). A well-known example of non-thermal desorption in a disk is the detection of CH_3OH in the disk of TW Hya (Walsh et al. 2016; Ilee et al. 2026).

Whereas freeze-out and sublimation directly affect the observed molecular reservoirs, it is the processes that happen on the grains themselves that are of crucial importance in the formation of molecular species. Their initial formation is dominated by the addition of atomic hydrogen (Hasegawa et al. 1992). This process has been very important in the formation of H_2 (Gould & Salpeter 1963; Wakelam et al. 2017), H_2O (hydrogenation of atomic oxygen; Tielens & Hagen 1982), and species like H_2CO and CH_3OH (hydrogenation of CO; Watanabe & Kouchi 2002; Fuchs et al. 2009; Santos et al. 2022). Grain-surface processes can also lead to the formation of more complex species, involving radicals following photodissociation or hydrogen abstraction events.

Crucial for the efficiency of grain-surface chemistry is the notion that grain-surface reactions are effectively three-body processes, which is in stark contrast with the gas-phase processes. Here, the grains are the third body and act as catalysers by absorbing the energy released by bond formation.

1.4 This thesis

With the recent launch of JWST and the ongoing studies with ALMA, the chemistry in both the inner (<10 au) and outer (>10 au) regions of planet-forming disks can be studied in great detail. Constraining the chemical composition in both regions is crucial for our understanding of the chemical evolution of these systems, and, in particular, the composition of the emerging planets. Radial drift and substructures play a key role in this regard, as they can directly influence the observable chemistry. This thesis focuses, therefore, on the chemical compositions in both regions and investigates the role of both drift and structure in setting the

chemistry. Subsequently, the thesis is subdivided into three parts: the first part (Chapters 2, 3, and 4) focuses on the inner disk physical structure and chemistry using new data from the JWST/MIRI through the MINDS collaboration, the second part (Chapter 5) focuses on high-resolution ALMA observations to hunt for substructures in the outer disk, and the third and final part (Chapters 6 and 7) focuses on the outer disk chemistry. A summary of each of the chapters and the main conclusions is provided below.

Chapter 2. *MINDS: The DR Tau disk. I. Combining JWST-MIRI data with high-resolution CO spectra to characterise the hot gas*
This chapter focuses on the JWST spectrum of the IR bright disk of DR Tau, revealing strong emission signatures of CO, H_2O (the focus of Chapter 3), OH, CO_2, HCN, and C_2H_2. High spectral resolution, ground-based observations of IRTF-iSHELL and VLT-CRIRES were used to analyse the excitation conditions of CO, which were also able to describe the MIRI observations. This suggests that the ground-based and JWST observations can be used in tandem to explore the conditions in the inner regions. Based on derived temperatures and emitting areas, the emission structure of the disk was revealed: CO emits from the hot, innermost regions of the disk, even from inside the dust sublimation radius. HCN and C_2H_2 are expected to emit from a deeper layer in the disk, whereas CO_2 emits from even deeper or further out. Additionally, the CO observations suggests that the inner disk may be misaligned with respect to the outer disk.

Chapter 3. *MINDS: The DR Tau disk. II. Probing the hot and cold H_2O reservoirs in the JWST-MIRI spectrum*
The H_2O emission observed with JWST-MIRI/MRS can be subdivided into the ro-vibrational transitions emitting at the shorter wavelengths (<10 μm) and the pure rotational transitions at longer wavelengths (>10 μm). The emission traces a radial gradient in the disk, where the temperature decreases with wavelength, while the emitting radius increases. Three different reservoirs can be distinguished using the pure rotational H_2O transitions: hot (T $\sim$800 K), warm (T $\sim$470 K), and cold (T $\sim$180 K). The cold component may be enhanced by drifting icy pebbles crossing the snowline, however, this could not be confirmed. Crucially, a comparison between the derived abundances (i.e., the total number of molecules) of H_2O and CO ($\mathcal{N}_{H_2O}/\mathcal{N}_{CO}$ $\sim$0.17) suggests that the H_2O abundance may be slightly depleted.

Chapter 4. *MINDS: Water reservoirs of compact planet-forming dust disks: A diversity of H_2O distributions*
To investigate the potential role of radial drift in enhancing the gaseous cold H_2O reservoir, this chapter focuses on analysing the pure rotational transitions of a sample of 8 compact disks (R_{dust} $\lesssim$60 au). By investigating the strengths of the different rotational H_2O reservoirs and deriving line ratios that trace their respective strengths, it was found that only two of the eight disks show strong cold H_2O emission. This reservoir may be enhanced due to radial drift in these two disks, but accretion variability could not be ruled out. Four of the other disks show

strong emission from all three components, but the cold reservoir is not enhanced. The spectra of the final two disks are dominated by other molecules (such as CO_2), and only show weak emission the rotational H_2O transitions. The weakness of the H_2O reservoirs may be the result of a (small) inner cavity.

The main results of Part 1 of this thesis, the chemical and physical structure of the inner disk, can be summarised as follows:

- High-resolution, ground-based observations of CO are crucial for deriving the excitation temperature, column density, and emitting radius. Additionally, they can be used to study potential misalignments between the inner and outer disk. (Chapter 2)
- The pure rotational H_2O transitions observed with JWST-MIRI/MRS can be attributed to three different reservoirs: hot, warm, and cold. The strengths of these reservoirs may reveal whether the H_2O is enhanced near the snow-line (following, for example, radial drift or accretion variability) or if the reservoirs are depleted (due to, for example, an inner cavity). (Chapter 3 and 4)
- Not all compact disks are enhanced in their cold H_2O reservoirs due to efficient radial drift. (Chapter 4)

Chapter 5. *MINDS: The influence of outer dust disk structure on the volatile delivery to the inner disk*
This chapter is part of Gasman et al. (2025). The main goal of this study was to investigate the influence of outer disk substructures on the volatile delivery by radial drift to the inner disk. Through a visibility fitting approach, archival high-resolution ALMA observations were analysed to hunt for substructures that could not be seen in the image plane. The found substructures include a small inner cavity in the disk of BP Tau. No direct connection between the inferred substructures and inner disk reservoirs - in particular, that of H_2O - could be established. As an example, a deep gap in the inner regions of Sz 98 was found, yet this disk also showed the strongest cold H_2O reservoir, suggesting that the gap may be leaky to gas and small dust grains.

The main results of Part 2, the outer disk structure, are as follows:

- ALMA visibility fitting techniques are a powerful tool to study substructures at small radial locations. A small sample of 8 disks reveals that substructures at distances of $\lesssim$15 au may be a common occurrence. (Chapter 5)

Chapter 6. *Characterising the molecular line emission in the asymmetric Oph-IRS 48 dust trap: Temperatures, timescales, and sub-thermal excitation*
The Oph-IRS 48 disk is an interesting laboratory to study the role of its azimuthally asymmetric dust trap in setting the observable chemistry. Using the many observed transitions of SO_2, H_2CO, and CH_3OH, the goal of this chapter was to constrain the excitation conditions at the location of the dust trap. No

thermal signatures of a vortex trapping the dust particles were found. Through a rotational diagram analysis, it was found that both CH_3OH and H_2CO are subthermally excited, pointing to them being located in the lower density upper layers of the disk. Conversely, SO_2 is seen to be thermally excited, which implies that its emission originates from a layer close to the midplane. The photodissociation timescales reveal that both CH_3OH and H_2CO must be rapidly dissociated ($\tau_{\rm pd}$ <1 year). Crucially, the photodissociation products of CH_3OH (and H_2O and CH_4) are needed in the gas-phase formation of H_2CO, suggesting that two reservoirs of H_2CO may be present, which can also explain its somewhat larger azimuthal distribution: one reservoir due to the sublimation of ices, another due to efficient gas-phase formation.

Chapter 7. *The asymmetric carbon-rich chemistry of the planet-forming disk of HD 142527 triggered by late infall*
Using new ALMA observations in tandem with archival observations, this chapter focuses on the molecular asymmetries in the disk of HD 142527. The majority of the azimuthal asymmetries can be explained by late infall. The infalling material is thought to replenish the disk with fresh atomic carbon that locally enhances the C/O-ratio and causes the efficient gas-phase formation of hydrocarbons (such as C_2H), CN, and CS. Furthermore, the infalling material may also have triggered the instability that created the dust asymmetry and may be the cause of a co-spatial enhancement in the gas surface density.

The main results and conclusions of part 3, the chemical composition of the outer disk, can be summarised as follows:

- The emission of CH_3OH and H_2CO in the disk of Oph-IRS 48 originates from a small radial sliver near the inner edge of the dust trap and is subthermally excited due to the lower gas density of the emitting upper layer. The emission of SO_2 originates from a layer close to the midplane, based on its thermal excitation requiring a high density. (Chapter 6)

- The rapid photodissociation of CH_3OH, H_2O, and CH_4 in the elevated emitting layers of Op-IRS 48 may facilitate efficient gas-phase formation of H_2CO. (Chapter 6)

- The chemical composition in the outer disk of HD 142527 is not dominated by the large asymmetric dust trap or the shadows observed in scattered light due to the misaligned inner disk. Instead, it may be set by late infalling material. (Chapter 7)

- Observing molecules like CN, C_2H, and H_2CO in disks with spiral-like features may reveal unique insights into the role of infalling material in setting the outer disk composition. (Chapter 7)

1.4.1 Future prospects

The high sensitivity and resolution observations of JWST and ALMA now provide unique insights into the chemical composition from the inner to outer disk. To improve our understanding of the (chemical and physical) processes dominating the chemistry, future studies should focus on combining these observations. To study the chemistry across the full disks, we need to constrain both the physical and thermal structures within the disks. Both existing and future telescopes give us the means to achieve this, especially since the future of observationally studying planet-forming disks is bright.

The flawless launch of JWST has opened up the possibility of extending the mission from its original 10 years to 20 years. If no complications arise, the telescope will remain operational for over a decade, yielding ample time opportunity to continue studying the inner disk compositions. More observations of different environments, such as disks with high UV irradiation or disks in binary systems, may yield more insights into the curious differences between the C-rich inner disks of VLMS stars and the more O-rich T-Tauri disks. Furthermore, this allows for time-domain studies to take place, where re-observing a disk or making use of the introduced Long-Term Monitoring Initiative would allow for variability studies following, for example, variable accretion and/or accretion outbursts.

With ALMA already having been operational for over a decade, it has revolutionised our understanding of the outer disk chemistry. The doubling of the bandwidth during the upcoming ALMA Wideband Sensitivity Upgrade (WSU; Carpenter et al. 2023) will target many more molecular transitions in a single observation. This is of particular interest for observations of C_2H, as its transitions are not close in frequency space to commonly observed species, such as the CO isotopologues. Therefore, we will gain a lot more information on the chemical composition and elemental ratios of many disks in the not-too-distant future.

As the construction of the ELT is well underway, high-resolution and sensitivity observations with the integral field unit of METIS (Brandl et al. 2021) are on the horizon. METIS will not only achieve high spectral resolution ($R \sim$100,000) that will be crucial for inferring the inner disk conditions and structures through the ro-vibrational CO transitions, but it also has a high spatial resolution ($\sim$0.03") that can directly reveal gas substructures in the bright Herbig disks. The observations also yield the opportunity to study the ro-vibrational bands of CO isotopologues, ^{13}CO and $C^{18}O$, and additional bands of H_2O, HCN, C_2H_2, and CH_4. By combining these data with JWST observations, the inner disk chemical abundances may be further constrained.

While there are presently no operational FIR telescopes, this may be changed in the near future by the potential missions POEMM and PRIMA. POEMM is a proposed balloon mission that would observe a subset of disks in a 20-day flight through the Antartic skies. PRIMA is, on the other hand, one of the final candidates for an upcoming NASA probe mission and has many crucial science goals (see, for example, Banzatti et al. 2025a; Pontoppidan et al. 2025; Salyk & Gasman 2025): constrain the gas mass using HD, to further investigate the cold H_2O reservoir, and to hunt for emission of $H_2\ ^{18}O$.